

## On the electronic density of states of age-hardening aluminium alloys

A Szasz†, L M Watson‡, L Kertesz† and J Kollart†

† Laboratory of Surface and Interface Physics, Eotvos University Budapest, Muzcum krt. 6-8, Budapest H-1088, Hungary

‡ Department of Metallurgy, University of Strathclyde, Glasgow, UK

Received 20 November 1987

**Abstract.** Changes in the electronic density of states (DOS) caused by plastic deformation and hydrostatic pressure in dilute Al-Mg-Si alloys are examined. Significant changes in the DOS were observed which depended on the mechanical treatment of the alloy. The observations are compared with the DOS of the same alloy in metastable states.

### 1. Introduction

At an early stage in his review on the internal structure of Guinier-Preston zones in alloys, Cohen [1] points out that the reason for the existence of metastable states is not clear. Obviously they must be associated with a local minimum in the free energy of the alloy to which strain energy in the lattice and chemical bond energy would contribute. These two factors are not unrelated and it has been shown both experimentally [2] and theoretically [3] that strain affects the Fermi surface of metals. In the present communication we demonstrate that plastic deformation and elastic strain can cause changes in the density of states (DOS) in an Al-Mg-Si age-hardening alloy, monitored by measuring the Al  $L_{2,3}$  soft x-ray emission spectrum (SXES) [4]. Further, we show that there is a similarity between the spectra from the elastically and plastically deformed samples and samples of the same alloy which have been heat treated to produce different metastable states [5]. The particular age-hardened state of the alloy was determined using differential thermal analysis (DTA) [6].

### 2. Experimental procedure

The composition of the age-hardening alloy studied was Al-Mg 0.64 wt%-Si 0.40 wt% and it was prepared by melting high purity (99.99%) components in an induction furnace. Samples were solution treated at 550 °C, quenched and subjected to a measured amount of plastic deformation by swaging and flattening. One SXES measurement was carried out on a solution-treated sample subjected to approximate hydrostatic pressure by clamping the sample in a vice during measurement. Age-hardened samples were also studied for comparison and these were prepared by suitable heat treatments in air prior to measurement. Two metastable states can be

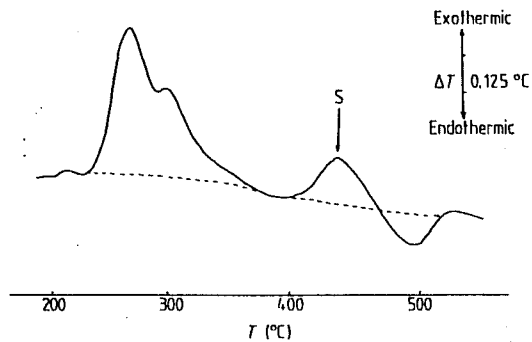


Figure 1. The DTA curve of the supersaturated alloy without deformation.

formed in this alloy, the first are coherent GP (Guinier–Preston) zones which form as needles in the  $\langle 100 \rangle$  directions and the second is  $\beta'$  which is hexagonal  $Mg_2Si$  and forms as rods semicoherent with the aluminium lattice, also in the  $\langle 100 \rangle$  directions [7]. DTA measurements were carried out on the supersaturated solid solutions after plastic deformation to determine the temperature of onset of the equilibrium precipitate.

### 3. Results

The DTA curve from the alloy in the solution treated and quenched condition without deformation is shown in figure 1 and is in good agreement with previous measurements [8]. The position of the exothermic DTA peak corresponding to the formation of the equilibrium precipitate is marked S in the figure and moves to lower temperatures linearly with the percentage of plastic deformation applied prior to the DTA measurements (curve A in figure 2). For high deformations the transformation temperature of the stable phase is lowered by almost 100 K. Microhardness measurements carried out on the plastically deformed specimens before the DTA measurements show the expected increase with percentage deformation except at high deformations where an additional hardening contribution appears to be superimposed on the strain hardening (curve B in figure 2).

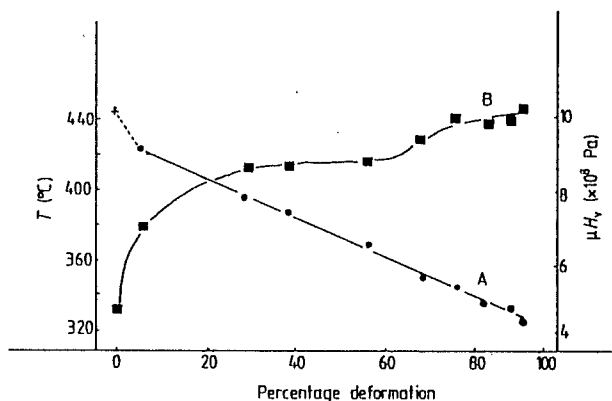


Figure 2. The deformation dependence of the microhardness (B) and of the DTA S-peak position (denoted in figure 1) (A) against the percentage plastic deformation ratio.

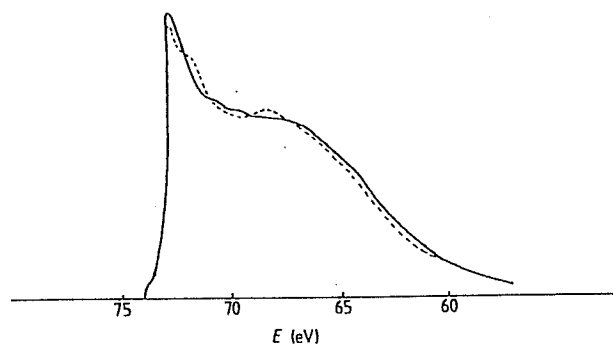


Figure 3. The SXES spectra of a plastically deformed alloy (full curve) and pure aluminium (broken curve).

The Al  $L_{2,3}$  SXES obtained from samples plastically deformed by 91% and from a sample subjected to an approximately homogeneous hydrostatic pressure are shown in figures 3 and 4. The spectrum from pure undeformed aluminium is also included for comparison [9]. On the assumption that the density of s and d electrons in the valence bands of the alloys remains unchanged in their different conditions, the spectra have been normalised on their integrated areas.

The most noticeable changes in the spectra occur in the half-band width (HBW) and in their shapes in the vicinity of 70 eV. The spectrum of the hydrostatically deformed sample has an emphasised peak at approximately 70 eV and the HBW is smaller than that of the aluminium reference while the HBW of the spectrum from the plastically deformed sample is larger than that of the reference. The SXES of the alloy in the GP and  $\beta'$  metastable states are displayed in figure 5. The  $L_{2,3}$  spectra of pure Al and Al 1 wt%  $Mg_2Si$  alloy in the stable undeformed state do not differ [10].

#### 4. Discussion

The diffusion-controlled formation of the stable intermetallic phase  $Mg_2Si$  will be promoted by strain fields in the lattice so the shift of the DTA peak (S) to lower temperatures with plastic deformation is not surprising, the linearity of the shift with

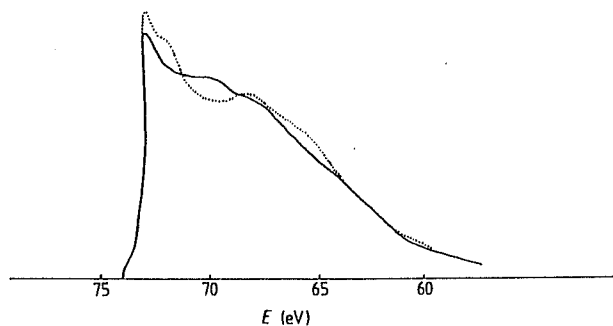


Figure 4. The SXES spectra of the hydrostatically compressed alloy (full curve) and pure aluminium (dotted curve).

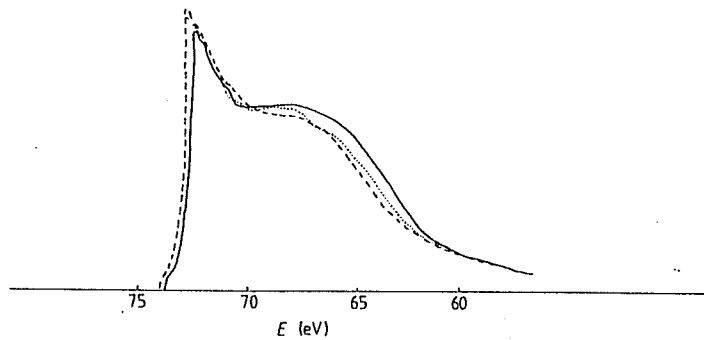


Figure 5. The SXE spectra of the alloy in the GP (full curve) and  $\beta'$  (broken curve) states and pure aluminium (dotted curve).

percentage deformation is, however, remarkable. Likewise, the shape of the microhardness against percentage deformation curve is as expected until very high deformations where age hardening at ambient temperatures probably contributes to the increase in hardness.

The measured SXES curves represent the *s* and *d* partial density of states (partial DOS) [11]. For Al and its dilute alloys the spectra can be discussed within the framework of the nearly-free-electron theory (NFE) [9]. Accepting this assumption, a free-electron parabola can be fitted to the low-energy region of the spectra with suitable allowance being made for many-body effects such as Auger broadening, plasmon satellites, etc. Deviations from the free-electron-parabola near the Fermi energy are due to a change in the density of states and change in symmetry due to the filling of the second and third Brillouin zones. This simple picture is complicated in alloys by hybridisation and bonding effects but these can with confidence be expected to be small in the present study because of the dilution of the alloys and the low atomic number of the components involved. For the same reasons the distribution of *p* states in the valence band of the alloys might be expected to remain more or less constant. Accepting these assumptions, the energy of the mass centre (MC) of the  $L_{2,3}$ -emission bands can be taken as a measure of the electronic contribution to the free energy of the alloys.

In previous publications [12, 13] we have shown that the MC moves to lower energies in aluminium alloys containing coherent GP zones, suggesting a strong electronic contribution to the metastability of this state. In this present study figure 5 shows a shift of the SXES to lower energies for the alloy containing GP zones which reverts to the pure metal position in the alloy containing the semicoherent  $\beta'$  precipitates in support of the previous statement. The GP zones, although coherent with the aluminium lattice, cause considerable internal stress due to variations in lattice parameter. The overall effects of this internal stress on the SXES are similar to the effects caused by the constant externally applied compressive stress on the supersaturated solid solution (figure 4) with the important difference that the external stress does not cause a shift of the spectrum to lower energies. Another noticeable difference in the spectra is the enhanced intensity in the externally stressed sample at around 70 eV which, in the nearly-free-electron model, would imply an increase in *s*-state density at the bottom of the second Brillouin zone. We can offer no explanation for this effect.

For the alloy heat treated to produce the semicoherent  $\beta'$  precipitates, internal stress will be relieved by the formation of partial grain boundaries but there will be an increase in internal strain. This sample should compare better with the cold-worked alloy and in fact this is the case. There is an increase in the emission intensity at the Fermi edge in both cases, suggesting an increase in the density of states in this region. This is in accord with the Brillouin-zone averaged calculations of Steinemann and Fischer [14] who concluded that plane strain caused by a high dislocation density considerably enhances the density of states at the Fermi level.

In this paper we show that internal stress and strain, whether applied externally or internally by zone formation, can have a considerable effect on the density of electron states and that this can be observed experimentally using soft x-ray emission spectroscopy. Further, it adds support to our previous conclusion [13] for the aluminium-silver system that the initial GP zone formation is stabilised by a lowering of the electronic contribution to the free energy of the alloy (full curve in figure 5), thus forming a local minimum. This contribution is not present to such an extent in the alloy with the  $\beta'$  precipitates and in this case a minimum in the free energy must be due to the configurational entropy term caused by the semicoherency of the precipitates.

### Acknowledgment

The financial support of Hungarian Ministry of Education is highly appreciated.

### References

- [1] Cohen J B 1986 *Solid State Phys.* **39** 131
- [2] Anderson J R, Papaconstantopoulos D A and Schirher J E 1981 *Phys. Rev. B* **24** 6790
- [3] Joss W and Monnier R 1980 *J. Phys. F: Met. Phys.* **10** 9
- [4] Szasz A, Kertesz L, Kojnok J, Kovacs M and Csik S Z 1983 *Vacuum TAIP* **33** 43
- [5] Kertesz L, Kojnok J and Szasz A 1982 *Cryst. Lattice Defects Amorph. Mater.* **9** 219
- [6] Hajdu J, Kertesz L, Lenart Cs and Nagy E 1974 *Cryst. Lattice Defects Amorph. Mater.* **5** 177
- [7] Polmear I J 1981 *Light Alloys, Metallurgy of Light Metals* (London: Edward Arnold)
- [8] Kertesz L, Lenart Cs and Kovacs-Treer M 1979 *Cryst. Lattice Defects Amorph. Mater.* **8** 99
- [9] Rooke G A 1968 *J. Phys. C: Solid State Phys* **1** 767
- [10] Kertesz L, Kojnok J, Szasz A and Sulakov A S 1981 *Recent Developments in Condensed Matter Physics* vol. 2 ed. J T Devreese *et al* (New York: Plenum) p 95
- [11] Rooke G A 1968 *Soft X-ray Band Spectra and Electronic Structure of Materials* ed. D J Fabian (London: Academic)
- [12] Szasz A, Kertesz L, Kojnok J, Hajdu J and Kollar J 1985 *Aluminium* **61** 515
- [13] Negm N, Watson L M and Szasz A 1987 *Proc. X-87 Int. Conf. on X-ray and Inner Shell Processes, Paris (J. Physique to be published)*
- [14] Steinemann S G and Fischer E S 1981 *Electronic Structure and Properties (Treatise on Material Science and Technology* vol. 21) ed. F Y Fradin (New York: Academic)